Nuclear Science and Techniques **24** (2013) 050503

Constraints on symmetry energy and *n*/*p* effective mass splitting with improved quantum molecular dynamics model

ZHANG Yingxun[1,2,*] LI Zhuxia[1] ZHAO Kai[1] LIU Hang[3] TSANG M B[2]

[1]*China Institute of Atomic Energy, Beijing 102413, China*

[2]*National Superconducting Cyclotron Laboratory, Michigan State University, East Lansing, MI 48824, USA*

[3]*Texas Advanced Computing Center, University of Texas, Austin, Texas 78758, USA*

Abstract A new version of improved quantum molecular dynamics model that includes standard Skyrme interactions has been developed. Based on the new code, four commonly used parameter sets, SLy4, SkI2, SkM* and Gs are adopted in the improved quantum molecular dynamics model and the isospin sensitive observables, namely isospin transport ratios, single and double ratios of the yields of neutrons and protons are investigated. The isospin transport ratios are strongly sensitive to the slope of symmetry energy, and are not very sensitive to the nucleon effective mass splitting. On the other hand, the high energy neutrons and protons yields ratios from reactions at different incident energies provide a good observable to the momentum dependence of nucleon effective mass splitting. By comparing our calculations with the data, we find that the constrained L value (the slope of density dependence of symmetry energy) is about ~46 MeV when the Skyrme type interaction is considered in transport models, and the isospin diffusion data prefer to $m_n^* > m_p^*$, but it is not a strong constraint with deep χ^2 minimum.

Key words Symmetry energy, Nucleon effective mass splitting, Heavy ion collisions, ImQMD

1 Introduction

Knowledge about the symmetry energy which is defined as the difference in the binding energy between the pure neutron matter and symmetric nuclear matter is important for understanding not only the nuclear structure and nuclear reactions but also many critical issues in astrophysics. Recent observables used to constrain the symmetry energy range from isospin diffusions in heavy ion collisions (HIC)[1-14], to experiments that measure nuclear properties such as neutron skin, Pygmy Dipole Resonance, masses of Isobaric Analog States, and nuclei masses in Finite Range Droplet Model[15-24]. Until now, a general consensus on the symmetry energy, S_0, at saturation density and its slope, L ($L = 3\rho_0 dS(\rho)/d\rho|_{\rho=\rho_0}$, where $S(\rho)$ is the density dependence term of the symmetry energy), were obtained. But, the results still have large uncertainty and it needs further constraints.

The constraints from heavy ion collisions are obtained by comparing the data of isospin sensitive observables with the predictions from transport models which include the density dependence of symmetry energy as an input variable. Tighter constraints can be obtained from improved experiments or from improved theoretical models by including the missing physics.

In addition to the dependence on nuclear density, the symmetry potential also depends on the momentum of the nucleons in the system. Such dependence leads to the splitting of the nucleon effective mass, especially in the high density regions. An interesting new question arises as to whether the effective mass for neutrons (m_n^*) is higher than, equal to, or lower than that for protons (m_p^*), and how does the effective mass splitting changes with the momentum of nucleon. In fact, our lack of reliable knowledge about the neutron-proton effective mass splitting has been hindering the accurate extraction of $S(\rho)$ from nuclear reactions by using transport models,

Supported by National Natural Science Foundation of China (NSFC) projects (Nos. 11075215, 10875031, 11005022, 11005155 and 11275052), 973 Program of China (No. 2013CB834404) and National Science Foundation (Grants No. PHY-0606007).

* Corresponding author. *E-mail address:* zhyx@ciae.ac.cn

Received date: 2013-06-27

because the compressed nuclear system is excited due to violent nucleon-nucleon collisions and the contributions from the momentum dependence of symmetry potential cannot be entirely described with local density approximation[1,25,26]. There are some efforts on constraining the nucleon effective mass splitting by analyzing nuclei optical potential data[1,27], and the $m_n^* < m_p^*$ has been ruled out around normal density and Fermi momentum. Furthermore, it would be interesting and important to give constraints on the momentum dependence of effective mass splitting from heavy ion collisions data. In this paper, we investigate such dependence in a transport model by choosing different Skyrme effective nucleon-nucleon interactions.

2 New version of ImQMD

The Quantum Molecular Dynamics Model (QMD) represents the individual nucleons as Gaussian "wave-packet" with mean values that move in according the Ehrenfest theorem; i.e. Hamilton's equations[8]. At China Institute of Atomic Energy (CIAE), we developed and successfully applied a new QMD code, labeled ImQMD which includes mean field potentials calculated using a Skyrme energy density function with options for different forms of the density dependence of the symmetry potential, to study heavy ion reactions ranging from Coulomb barrier to 400 MeV per nucleon[28]. With these modifications, ImQMD has successfully described the multiplicity of reaction products, collective flows and stopping powers in intermediate energy Heavy Ion Collisions (HICs), but this version lacked to consider the nucleon effective mass splitting.

We improve the mean field part of the Improved Quantum Molecular Dynamics (ImQMD05) code by including the isospin dependent Skyrme like momentum dependence interaction as the form $u_{md} \propto \int dpdp' f(r,p) f(r,p')(p-p')^2$. The form of u_{md} is

$$\begin{aligned} u_{md} &= u_{md}(\rho\tau) + u_{md}(\rho_n\tau_n) + u_{md}(\rho_p\tau_p) \\ &= C_0 \int d^3pd^3p' f(r,p) f(r,p')(p-p')^2 \\ &\quad + D_0 \int d^3pd^3p' [f_n(r,p) f_n(r,p')(p-p')^2 \\ &\quad + f_p(r,p) f_p(r,p')(p-p')^2], \end{aligned} \tag{1}$$

where f is the nucleon phase space distribution function:

$$f = \sum_i \frac{1}{(\pi\hbar)^3} \exp\left(-\frac{(r-r_i)^2}{2\sigma_r^2}\right) \exp\left(-\frac{(p-p_i)^2}{2\sigma_p^2}\right), \tag{2}$$

$$f_n = \sum_{i\in n} \frac{1}{(\pi\hbar)^3} \exp\left(-\frac{(r-r_i)^2}{2\sigma_r^2}\right) \exp\left(-\frac{(p-p_i)^2}{2\sigma_p^2}\right), \tag{3}$$

$$f_p = \sum_{i\in p} \frac{1}{(\pi\hbar)^3} \exp\left(-\frac{(r-r_i)^2}{2\sigma_r^2}\right) \exp\left(-\frac{(p-p_i)^2}{2\sigma_p^2}\right). \tag{4}$$

The coefficients C_0 and D_0 can be determined with following relationship:

$$C_0 = \frac{1}{16\hbar^2}[t_1(2+x_1) + t_2(2+x_2)], \tag{5}$$

$$D_0 = \frac{1}{16\hbar^2}[t_2(2x_2+1) - t_1(2x_1+1)]. \tag{6}$$

In the new version of ImQMD code (ImQMD-Sky), the potential energy U is

$$U = U_{\rm loc} + U_{\rm md} + U_{\rm coul}. \tag{7}$$

The nuclear contributions are represented in a form with $U_{\rm loc,md} = \int u_{\rm loc,md} d^3r$. The energy density $u_{\rm loc}$ is

$$\begin{aligned} u_{\rm loc} &= \frac{\alpha}{2}\frac{\rho^2}{\rho_0} + \frac{\beta}{\beta+1}\frac{\rho^{\eta+1}}{\rho_0^\eta} + \frac{g_{\rm sur}}{2\rho_0}[\nabla\rho]^2 \\ &\quad + \frac{g_{\rm sur,iso}}{\rho_0}\left[\nabla(\rho_n-\rho_p)\right]^2 \\ &\quad + A_{\rm sym}\rho\delta^2\rho + B_{\rm sym}\rho^\eta\delta^2\rho. \end{aligned} \tag{8}$$

Here, δ is the isospin asymmetry. $\delta=(\rho_n-\rho_p)/(\rho_n+\rho_p)$, ρ_n and ρ_p are the neutron and proton densities, respectively. The coefficients of α, β, $g_{\rm sur}$, $g_{\rm sur,iso}$, $A_{\rm sym}$ and $B_{\rm sym}$ can be obtained by the standard Skyrme interaction parameters as in previous work[28]. $U_{\rm coul}$ is Coulomb energy. The mean fields acting on these wavepackets are derived from potential energy.

These calculations use isospin-dependent in-medium nucleon-nucleon scattering cross sections in the collision term and Pauli blocking effects as described in Ref.[28]. With this new version of Improved Quantum Molecular Dynamics code, we can directly test the validity of Skyrme interaction parameters which have been wildly used in nuclear structure studies in heavy ion collisions, and provide constraints on the density dependence of symmetry energy and *n*/*p* effective mass splitting.

Based on the Skyrme interaction, one can get

the density dependence of symmetry energy, neutron and proton effective mass and the symmetry potential for cold nuclear matter on the mean-field level as follows:

$$S(\rho)=\frac{1}{3}\frac{\hbar^2}{2m}\rho_0^{\frac{2}{3}}\left(\frac{3\pi^2}{2}\frac{\rho}{\rho_0}\right)^{\frac{2}{3}}+A_{\rm sym}\rho + B_{\rm sym}\rho^{\eta}+C_{\rm sym}\rho^{5/3}, \quad (9)$$

$$\left(m_\tau^*/m\right)^{-1}=[1+4(C_0\rho+D_0\rho_\tau)m], \quad (10)$$

$$U_{\rm sym}=\frac{U_n-U_p}{2\delta}=2A_{\rm sym}\rho+2B_{\rm sym}\rho^{\eta}+2D_0m\rho E_k. \quad (11)$$

Eq.(9) is the density dependence of symmetry energy for cold nuclear matter, the first term comes from the contribution of kinetic energy part, the second and third terms are from the two-body and three body terms in Skyrme interactions. The last term in Eq.(9) comes from the momentum dependent interaction term in Skyrme interaction, and $C_{\rm sym}$ is determined as in Ref.[28]. Eq.(10) is the effective mass where ρ_τ is the neutron or proton density for $\tau=n, p$. Eq.(11) is the symmetry potential also known as the Lane potential which gives the strength of the symmetry potential in asymmetric nuclear matter.

3 Results and discussion

In the following studies, we choose four Skyrme interaction parameter sets, SLy4, SkI2, SkM* and Gs which have similar effective mass and incompressibility[29-32], i.e., m^*~0.7±0.1, K_0=230±20 MeV, and have been widely used in the studies of nuclear structure and neutron star. The SLy4 and SkI2 were fitted to properties of neutron matter, neutron star and the ground-state variables of neutron-rich heavy nuclei, and the neutron effective mass is less than the proton effective mass, $m_n^*<m_p^*$. We choose these two interactions because the slopes of symmetry energy L are very different; L is 46 MeV for SLy4, and 104 MeV for SkI2. The SkM* and Gs were fitted to binding energies of finite nuclei and actinide fission barriers, and the neutron effective mass is larger than the proton effective mass, $m_n^*>m_p^*$. L for SkM* is 46 MeV, and 93 MeV for Gs. By analyzing the results from calculations using SLy4, SkI2, SkM* and Gs and comparing to data, we hope to understand the sensitivities of the interactions on the density dependence of symmetry energy and neutron proton effective mass splitting simultaneously and get their constraints. In this paper, we focus our discussion on the ^{112,124}Sn+^{112,124}Sn reactions at 50A MeV which have been measured in the MSU/NSCL group.

Figure 1 shows the density dependence of symmetry energy (left panel) and the energy dependence of the Lane potential (right panel), for cold nuclear matter. At subsaturation density, the strengths of symmetry energy obtained with SLy4 (top solid lines) and SkM* (bottom solid line) are stronger than that obtained with SkI2 (top dashed lines) and Gs (bottom dashed lines). Separation of the two groups of (solid and dashed) lines is strongly correlated with the L values. Smaller L values yield higher symmetry energy at subsaturaion densities while the opposite is true at the suprasaturation density regions. The right panels of Fig.1 show the Lane potentials for the above four interactions at $0.5\rho_0$ (top panel) and at ρ_0 (bottom panel) as a function of nucleon kinetic energy. The energy dependence of symmetry potential for SLy4 and SkI2 are positive and increase with the energy of nucleons. However, those for SkM* and Gs decrease with the kinetic energy and become negative above 200 MeV. When $m_n^*<m_p^*$, as in the case of SLy4 and SkI2, the neutrons feel stronger repulsion than protons and the effects increase with the kinetic energy increasing. The opposite is true for SkM* and Gs where $m_n^*>m_p^*$, the protons feel stronger repulsion with the kinetic energy increasing.

The symmetry potential (Lane potential) also gives an accurate estimate for the difference of the force between neutron and proton feeling in asymmetric nuclear matter, and directly influences the n/p ratios of emitted nucleons. The larger the Lane potential is, the larger the n/p ratio is. At high energy, one can expect that the n/p ratios with $m_n^*<m_p^*$ are greater than that for $m_n^*>m_p^*$ because the Lane potential for $m_n^*<m_p^*$ is larger than that for $m_n^*>m_p^*$ cases. Furthermore, we can see that a crossing of two symmetry potentials for SLy4 and SkM* appears at $E_k^{\rm crossing}\sim 30$ MeV for $\rho=0.5\rho_0$ and $E_k^{\rm crossing}\sim 70$ MeV for $\rho=\rho_0$. Below the crossing energy, the Lane potential for $m_n^*<m_p^*$ cases is less than that for $m_n^*>m_p^*$, we can expect that the n/p ratios with

$m_n^* < m_p^*$ are less than that for $m_n^* > m_p^*$ if their differences on the Lane potential are large enough.

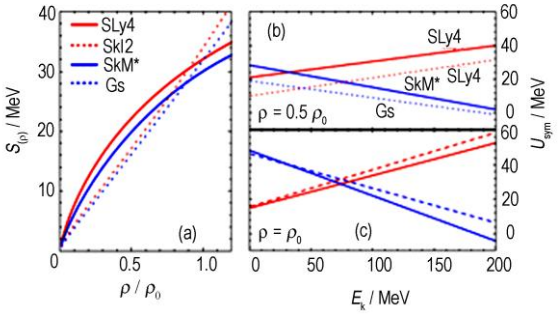

Fig.1 (Color online) (a) Density dependence of symmetry energy, (b) Energy dependence of the Lane potential at ρ=0.5ρ_0 and (c) ρ=ρ_0, for the parameters SLy4 (red solid lines), SkI2 (red dashed lines), SkM*(blue solid lines), Gs (blue dashed lines).

Before analyzing the isospin sensitive observables, we firstly check the calculated results on charge distribution for ^{124}Sn+^{124}Sn with ImQMD-Sky. Fig.2 shows the charge distributions for ^{124}Sn+^{124}Sn at E_{beam}=50A MeV obtained with four Skyrme parameter sets, SLy4, SkI2, SkM* and Gs. It is clear that the charge distribution, which is considered as an isoscalar observable, is weakly sensitive to the slope of symmetry energy and nucleon effective mass splitting among the selected parameters.

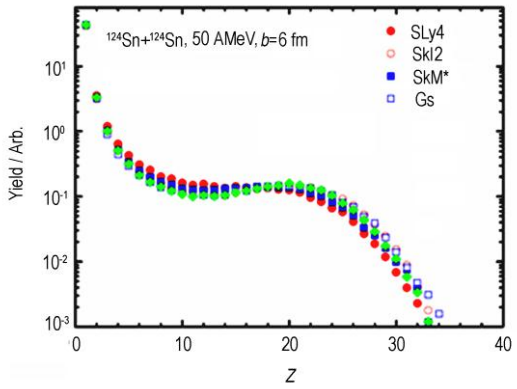

Fig.2 (Color online) Charge distributions for ^{124}Sn+^{124}Sn at E/A=50 MeV and b=2 fm for four Skyrme parameter sets, SLy4, SkI2, SkM* and Gs.

In previous studies[3,6,8,9,11], the density dependence of symmetry energy has been probed using peripheral collisions to measure the isospin diffusion and isospin transport ratios as a function of rapidity. Moreover, even though there are data from n/p yield ratios and flow, the constraints on the symmetry energy from heavy ion collisions rely heavily on isospin diffusion data[6,11].

In this paper, we simulated the collisions of ^{124}Sn+^{124}Sn, ^{124}Sn+^{112}Sn, ^{112}Sn+^{124}Sn, and ^{112}Sn+^{112}Sn reactions at beam energy of 50 MeV per nucleon using the ImQMD-Sky code. 64,000 events are obtained for each reaction at b=6 fm. In the left panel of Fig.3, we plot the isospin diffusion transport ratios obtained with SLy4, SkI2, SkM* and Gs interactions. As in previous studies[6,8], we analyze the amount of isospin diffusion by constructing a tracer from the isospin asymmetry of emitting source which includes all emitted nucleons (N) and fragments (frag) with the velocity cut ($v_z^{N,frag} > 0.5v_{beam}^{c.m.}$). The shaded regions are the isospin diffusion data obtained by constructing the isospin transport ratios with isoscaling parameter X=α, near the projectile rapidity regions. Faster equilibration occurs for smaller L values which correspond to larger symmetry energies at subsaturation density. Our results show that the R_i values for SLy4 (solid circle) and SkM* (solid squares), both with L=46 MeV, are smaller than those for SkI2 (open circle, L=104 MeV) and Gs (open square, L=93 MeV) with similar effective mass splitting. The overall effect of mass splitting on isospin diffusion is small. When $m_n^* < m_p^*$, the isospin diffusion process is accelerated at subsaturation densities due to the stronger Lane potential. R_i values increase in the order of R_i(Sly4: L=46 MeV, $m_n^* < m_p^*$)< R_i(SkM*: L=46 MeV, $m_n^* > m_p^*$)< R_i(SkI2: L=104 MeV, $m_n^* < m_p^*$)< R_i(Gs: L=93 MeV, $m_n^* > m_p^*$). By comparing to the data, we found that the R_i obtained with both SLy4 and SkM* (L=46 MeV) fall within the experimental uncertainties among the interactions we adopted. The data prefer the softer symmetry potentials with lower L values.

We also compare the results of the calculations to R_i as a function of the scaled rapidity $y / y_{beam}^{c.m.}$ with SLy4, SkI2, SkM* and Gs interactions as shown in the right panel of Fig.3. The star symbols in the right panel are experimental data obtained in Ref.[13] for peripheral collisions. This transport ratio was generated using the isospin tracer X=ln[Y(^{7}Li)/Y(^{7}Be)], where Y(^{7}Li)/Y(^{7}Be) is the yield ratio of the mirror nuclei, ^{7}Li and ^{7}Be[13]. For comparison, the ImQMD-Sky calculations of R_i(X=$\delta_{N,frag}$) are plotted as lines for b=6 fm. The interactions with smaller L values, SLy4 and SkM* (solid lines) agree with the

data better especially in the high rapidity region. However, χ^2 analysis suggests that the data fit the results from SkM* interactions with $m_n^* > m_p^*$ effective mass splitting. Current study show that the sensitivity of the isospin diffusion to slope parameter is consistent with previous studies but the sensitivity to effective mass splitting is not large.

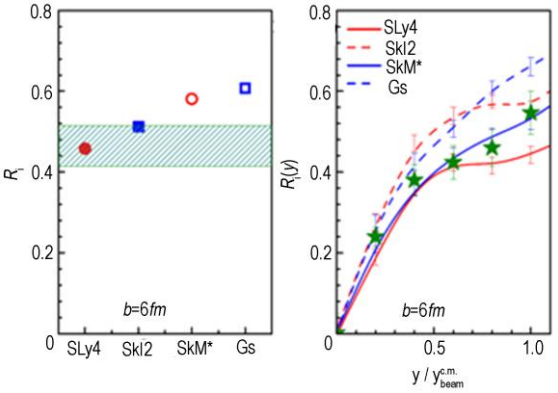

Fig.3 (Color online) Left panel: The isospin diffusion transport ratios obtained with SLy4, SkI2, SkM* and Gs. The shadow region is the data from Ref.[3]. Right panel: The calculated results on isospin transport ratios as a function of rapidity for SLy4, SkI2, SkM* and Gs. The star symbols are the data from Ref.[13].

Rizzo[26] has shown that the neutron/proton yield ratio, $Y(n)/Y(p)$, as a function of p_t from central collisions is a robust observable to study nucleon effective mass splitting. In Fig.4, we plot the $R(n/p)=Y(n)/Y(p)$ ratio for ^{112}Sn+^{112}Sn (left panel) and ^{124}Sn+^{124}Sn (middle panel) at b=2 fm with angular gate $70°<\theta_{\rm c.m.}<110°$. The lines connecting the solid and open circles correspond to $m_n^* < m_p^*$ case, and the lines connecting the squares correspond to $m_n^* > m_p^*$ case. Not surprisingly, the $Y(n)/Y(p)$ ratios are larger for the neutron rich system, ^{124}Sn+^{124}Sn, in the middle panel. Consistent with Refs.[26,27], the differences in the $Y(n)/Y(p)$ ratios between the $m_n^* < m_p^*$ (circles) and $m_n^* > m_p^*$ (squares) increase with kinetic energy of the nucleons. In this high energy region, the single ratios (left and middle panels) are more sensitive to the effective mass splitting than the isospin diffusion observables. This is because the contributions from momentum dependent part of symmetry potential play more and more important roles on the $Y(n)/Y(p)$ ratios when the relative momentum of nucleons increase. As shown in the right panel of Fig.1, the Lane potentials become larger for $m_n^* < m_p^*$ at high kinetic energy, and cause enhanced neutron emissions. Thus, the information about the momentum dependence of nucleon effective mass splitting is contained in the energy spectral of pre-equilibrium transverse emission of nucleons at earlier stage of reactions.

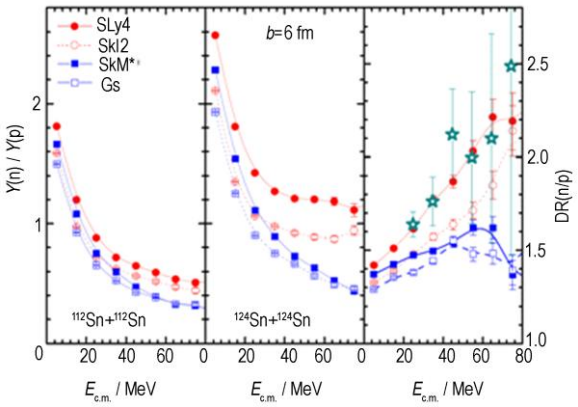

Fig.4 (Color online) Left panel is the calculated results for $Y(n)/Y(p)$ as a function of kinetic energy for ^{112}Sn+^{112}Sn at b=2 fm with angular cuts $70^o<\theta_{\rm c.m.}<110^o$; middle panel is the $Y(n)/Y(p)$ for ^{124}Sn+^{124}Sn. Right panel is the calculated results for $DR(n/p)$ ratios as a function of kinetic energy. The calculated results are for SLy4 (red solid lines), SkI2 (red dashed lines), SkM* (blue solid lines), Gs (blue dashed lines) and NRARP (green lines). Star symbols are the data[4].

The calculations with SLy4 interactions agree with the double ratios data [4], $DR(n/p)=(Y_A(n)/Y_A(p))/(Y_B(n)/Y_B(p))$, where A=^{124}Sn+^{124}Sn and B=^{112}Sn+^{112}Sn, from Ref.[4] which have very large uncertainties especially for ratios of the high energy nucleons. Thus，exact constraints on effective mass splitting from heavy ion collisions need re-measurements of the data with high quality. Since the effect of mass splitting should be larger at higher densities, most likely, one needs data on the $DR(n/p)$ ratios at different incident energies which should give more stringent constraints on the momentum dependence of n/p effective mass splitting by comparing with improved transport models calculations.

4 Conclusion

In summary, we have used a new version of the improved quantum molecular dynamics code, which can accommodate Skyrme interaction parameters, to study the isospin sensitive observables, such as isospin diffusion, isospin transport ratios as a function of rapidity, single and double neutron proton yield ratios. We find that the neutron proton effective mass

splitting plays an important role on the *n*/*p* ratios of transverse emitted nucleons at high kinetic energy. The mass splitting affects isospin diffusion, but the effects are not strong. Our results show that the constrained L~46 MeV value. The isospin diffusion data prefer to the neutron effective mass is greater than proton effective mass, but it is not a strong constraint with deep χ^2 minimum. We also show that the single and double *n*/*p* ratios from high nucleon energies are more sensitive to the mass splitting effects. The results also suggest that the effective nucleon masses should be further studied at different incident energies. Finally new neutron and proton spectral data with much smaller uncertainties than previous data at different beam energies may allow one to determine the sign and the momentum dependence of the mass splitting.

References

1 Li B A, Chen L W, Ko C M. Phys Rep, 2008, **464**: 113−281.

2 Tsang M B, Friedman W A, Gelbke C K, *et al*. Phys Rev Lett, 2001, **86**: 5023−5026.

3 Tsang M B, Liu T X, Shi L, *et al*. Phys Rev Lett, 2004, **92**: 062701.

4 Famiano M A, Liu T X, Lynch W G, *et al*. Phys Rev Lett, 2006, **97**: 052701.

5 Ono A, Danielewicz P, Friedman W A, *et al*. Phys Rev C, 2003, **68**: 051601.

6 Tsang M B, Zhang Y X, Danielewicz P, *et al*. Phys Rev Lett, 2009, **102**: 122701.

7 Zhang Y X, Danielewicz P, Famiano M, *et al*. Phys Lett B, 2008, **664**: 145−148.

8 Zhang Y, Coupland D D S, Danielewicz P, *et al*. Phys Rev C, 2012, **85**: 024602.

9 Coupland D D S, Lynch W G, Tsang M B, *et al*. Phys Rev C, 2011, **84**: 054603.

10 Kumar S, Ma Y G, Zhang G Q, *et al*. Phys Rev C, 2011, **84**: 044620.

11 Chen L W, Ko C M, Li B A. Phys Rev Lett, 2005, **94**: 032701.

12 Li B A, Ko C M, Ren Z. Phys Rev Lett, 1997, **78**: 1644−1647.

13 Liu T X, Lunch W G, Tsang M B, *et al*. Phys Rev C, 2007, **76**: 034603.

14 Kohley Z, May L W, Wuenschel S, *et al*. Phys Rev C, 2010, **82**: 064601.

15 Warda M, Vinas X, Roca-Maza X, *et al*. Phys Rev C, 2010, **81**: 054309.

16 Chen L W, Ko C M, LI B A, *et al*. Phys Rev C, 2010, **82:** 024321.

17 Gaidarov M K, Antonov A N, Sarriguren P, *et al*. Phys Rev C, 2012, **85**: 064319.

18 Carbone A, Col`o G, Bracco A, *et al*. Phys Rev C, 2010, **81:** 041301.

19 Wieland O, Bracco A, Camera F, *et al*. Phys Rev Lett, 2009, **102**: 092502.

20 Piekarewicz J. Phys Rev C, 2011, **83**: 034319.

21 Dong J M, Zuo W, Gu J Z. Phys Rev C, 2013 **87**: 014303.

22 Danielewicz P and Lee J. Nucl Phys A, 2009, **818**: 36.

23 Liu M, Wang N, Li Z X, *et al*. Phys Rev C, 2010, **82**: 064306.

24 Moller P, Myers W D, Sagawa H, *et al*. Phys Rev Lett, 2012, **108**: 052501.

25 Rizzo J, Colonna M, Di Toro M. Phys Rev C, 2005, **72**: 064609.

26 Li B A, Das C B, Das Gupta S, *et al*. Phys Rev C, 2004, **69:** 011603.

27 Xu C, LI B A, CHEN L W. Phys Rev C, 2010, **82:**054607.

28 Zhang Y and Li Z, Phys Rev C, 2005, **71:** 024604; Phys Rev C, 2006, **74:** 014602; Phys Rev C, 2007, **75:** 034615.

29 Chabanat E, Bonche P, Haensel P, *et al*. Nucl Phys A, 1997, **627**: 710−746.

30 Reinhard P G and Flocard H. Nucl Phys A, 1995, **584:** 467−488.

31 Bartel J, Quentin P, Brack M, *et al*. Nucl Phys A, 1982, **386**: 79−100.

32 Friedrich J and Reinhard P G. Phys Rev C, 1986, **33**: 335−351.